ISSN 8755-6839

SCIENCE OF **TSUNAMI HAZARDS**

Journal of Tsunami Society International

Volume 29 Number 2 2010

THE EARTHQUAKE AND TSUNAMI OF 27 FEBRUARY 2010 IN CHILE – Evaluation of Source Mechanism and of Near and Far-field Tsunami Effects

George Pararas-Carayannis

Tsunami Society International, Honolulu, Hawaii 96815, USA

tsunamisociety@hawaiiantel.net

ABSTRACT

The great earthquake of February 27, 2010 occurred as thrust-faulting along a highly stressed coastal segment of Chile's central seismic zone - extending from about 33ºS to 37ºS latitude - where active, oblique subduction of the Nazca tectonic plate below South America occurs at the high rate of up to 80 mm per year. It was the 5th most powerful earthquake in recorded history and the largest in the region since the extremely destructive May 22, 1960 magnitude M_w9.5 earthquake near Valdivia. The central segment south of Valparaiso from about 34º South to 36º South had been identified as a moderate seismic gap where no major or great, shallow earthquakes had occurred in the last 120 years, with the exception of a deeper focus, inland event in 1939. The tsunami that was generated by the 2010 earthquake was highest at Robinson Crusoe Island in the Juan Fernández archipelago as well as in Talchuano, Dichato, Pelluhue and elsewhere on the Chilean mainland, causing numerous deaths and destruction. Given the 2010 earthquake's great moment magnitude of 8.8, shallow focal depth and coastal location, it would have been expected that the resulting tsunami would have had much greater Pacific-wide, far field effects similar to those of 1960, which originated from the same active seismotectonic zone. However, comparison of the characteristics of the two events indicates substantial differences in source mechanisms, energy release, ruptures, spatial clustering and distributions of aftershocks, as well as in geometry of subduction and extent of crustal displacements on land and in the ocean. Also, the San Bautista and the Juan Fernández Islands - ridges rising from the ocean floor – as well as the O'Higgins seamount/guyot may have trapped some of the tsunami energy, thus accounting for the smaller, far field tsunami effects observed elsewhere in the Pacific. Apparently, complex, localized structural anomalies and interactions of the Nazca tectonic plate with that of South America, can account for differences in the spatial distribution and clustering of shallow event hypocenters, as well as for seismic gaps where large tsunamigenic earthquakes could strike Chile's Central Seismic zone in the future.

Key Words: Tsunami, Chile, seismotectonics, Peru-Chile subduction, energy trapping.

1. INTRODUCTION

Continuous crustal deformation associated with ridge collision and oblique convergence of the Nazca tectonic plate with the continental block of South America in the central Chile region had caused substantial deformation and strain accumulation which culminated in the great earthquake of February 27, 2010 (Fig. 1). The quake caused several hundred deaths and injuries and great destruction to property. Shortly thereafter, a destructive tsunami impacted coastal towns and villages in south-central Chile and the Juan Fernández Islands. There was substantial tsunami damage at Talcahuano, Constitución, Concepcion, Dichato and Pichilemu. A Pacific-wide tsunami warning was issued for the countries bordering the Pacific Basin. Although the tsunami's source region was immediately to the north of the destructive 1960 event and there were many similarities, the far-field impact was not as severe as anticipated.

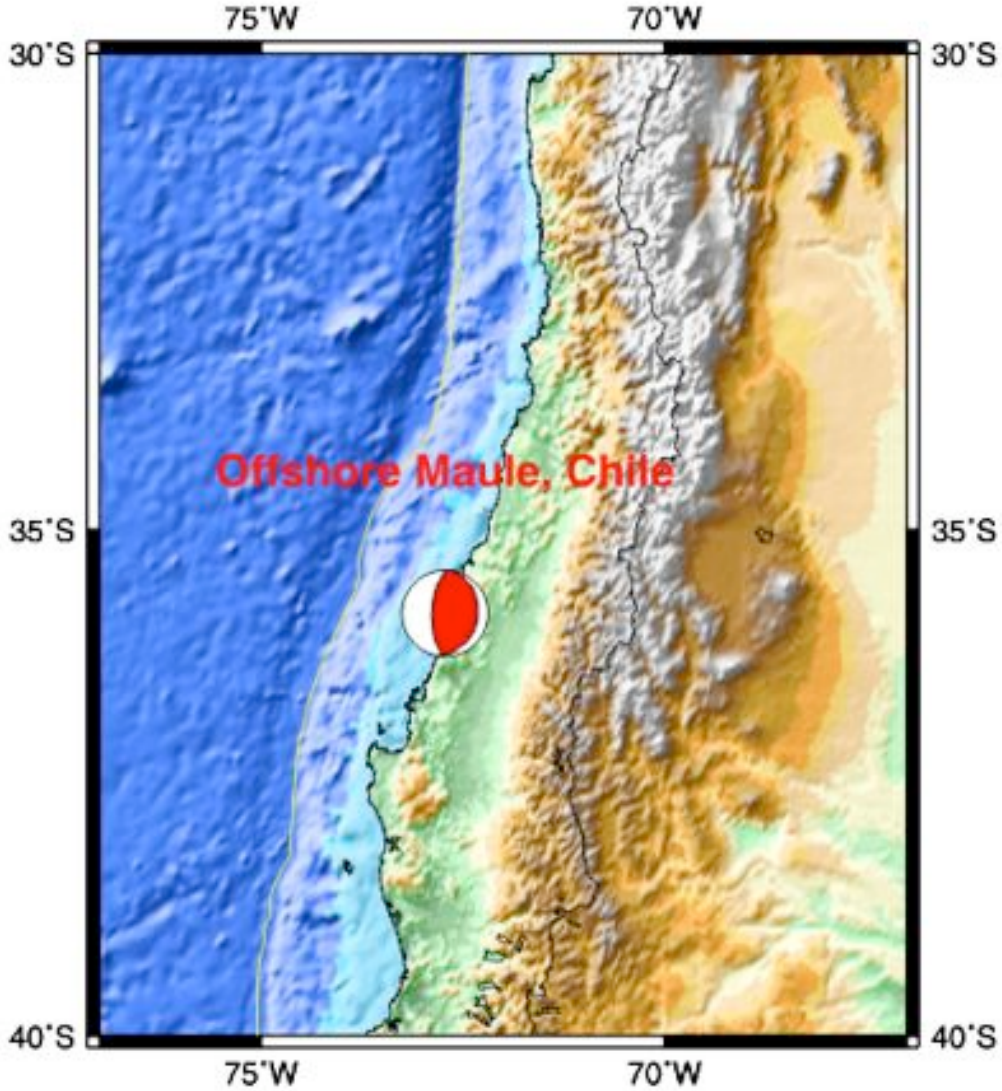

Fig. 1. Epicenter and focal mechanism of the Earthquake of 27 February 2010.

The present study examines the source characteristics of the February 27, 2010 earthquake and the possible reasons for the tsunami's less severe, far-field effects. Specifically examined are the seismotectonics of Chile's central seismic zone, the focal mechanism of the earthquake, the extent of ground and ocean floor displacements, the aftershock hypocenter space/time distribution, the geometry of subduction, the quake's tsunamigenic efficiency, the tsunami energy flux directivity, the absorption, trapping, reflection and ducting of wave energy by the Juan Fernández submarine ridge, the O'Higgins seamount and other submarine features and finally the potential for future destructive tsunamis from Chile's central seismic zone. Also, a comparison is made of similarities and differences of the source characteristics of the of February 27, 2010 tsunami with those of the destructive, Pacific-wide tsunami of May 22, 1960.

2. THE EARTHQUAKE

The Peru-Chile Trench is a manifestation of very active subduction along the South American continent. Most of the destructive tsunamis along the South American coast have been generated from major or great shallow earthquakes in close proximity to the Peru-Chile Trench. The great earthquake (magnitude Mw=8.8) that struck the Bio-Bio Province (population: 1.7 million) of Central Chile on early Saturday morning of February 27, 2010, 6:34:17 AM UTC (3:34 a.m. local time) was a subduction zone event which occurred as thrust-faulting near the interface of convergence, where the Nazca tectonic plate subducts landward below the South American continent plate at a rate of up to 80 mm per year. Its epicenter was at 35.909 S, 72.733 W offshore from Maule; 99 km (61 miles) of Talca; 117 km (73 miles) NNE of Concepción; and 317 km (197 miles) SW of Santiago. Its focal depth was given as 35 km. (21.7 miles) (USGS). Many cities in Maule region were seriously affected.

Aftershocks **-** A large vigorous aftershock sequence followed the main earthquake. There was unusual clustering of aftershocks in the first few minutes, which supports an anomalous rupture. An aftershock of M_w6.2 was recorded 20 minutes after the initial quake. A 6.9-magnitude offshore earthquake struck approximately 300 kilometers southwest less than 90 minutes after the initial shock; however, this may have been a separate event that may not have been related to the main shock. Two more aftershocks with magnitudes 5.4 and 5.6 followed within an hour. In the 2 1/2 hours following the 90-second main shock, 11 more were recorded. By March 1, 2010, a total of 121 aftershocks with magnitude 5.0 or greater were recorded (USGS NEIC). Eight of these had magnitudes of 6.0 or greater. By March 29, 2010, a total 458 aftershocks had been recorded. The significance of the aftershock distribution and of their spatial clustering as it relates to tsunami generation, is discussed in a subsequent section.

Rupture **-** The earthquake had a complicated rupture process. The total rupture was about 550 km long, more than 100 km wide and extended to about 50 km in depth. It paralleled the coast of Chile and affected an area of about 82,500 square kms.

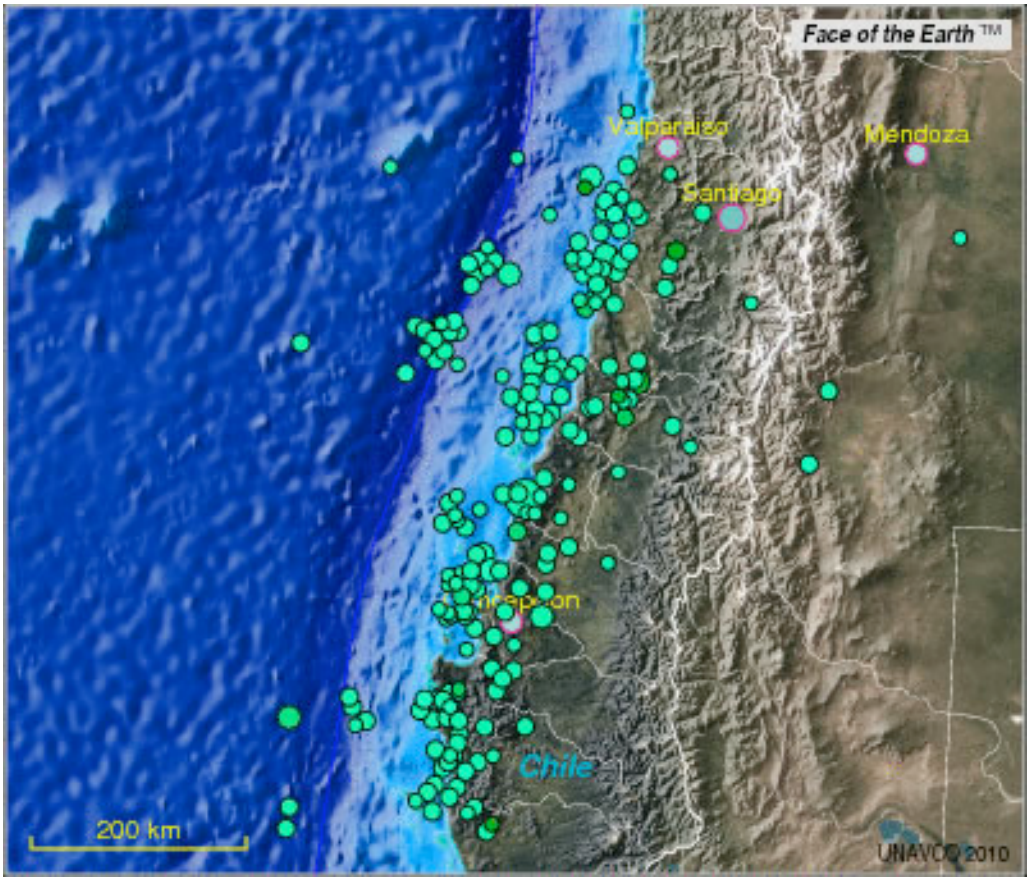

Fig. 2. Epicenter of the February 27, 2010 earthquake and distribution of aftershocks up to 18:00 UTC Mar 3. (Modified image from UNAVCO's Jules Verne Voyager).

Ground Motions and Earthquake Intensity - Ground shaking levels lasted for 90 seconds. Maximum acceleration of 0.65g was recorded at Concepción (USGS). The quake was strongly felt in six regions of Chile, from Valparaíso in the north to Araucanía in the south. The cities experiencing the strongest shaking were Concepción (IX) and Arauco and Coronel (VIII). In Santiago the intensity was VII. Intensities of VIII were experienced at Chiguayante, Coronel, Lebu, Nacimiento, Penco, Rancagua, Santiago, San Vicente, Talca, Temuco and Tome; Intensities of VII were felt from La Ligua to Villarrica and VI as far as Ovalle and Valdivia to the south. The quake was strongly felt in Argentina - including Buenos Aires, Córdoba, Mendoza and La Rioja - and in Ica in southern Peru about 2,400 km away. It was also felt in parts of Bolivia, southern Brazil, Paraguay, Peru and Uruguay (USGS).

Crustal Movements **-** Based on GPS Geodetic measurements, a team from Ohio State University and other institutions documented that the continental block moved westward. Specifically, it was determined that the city of Concepción moved 3.04 meters (10 ft) west, Santiago 28 centimeters (10 in) to the west-southwest and even Buenos Aires - about 1,350 kilometers (840 mi) from Concepción - moved westward by 3.9 centimeters (1.5 in). Maximum uplift of more than 2 m was observed along the coast Arauco.

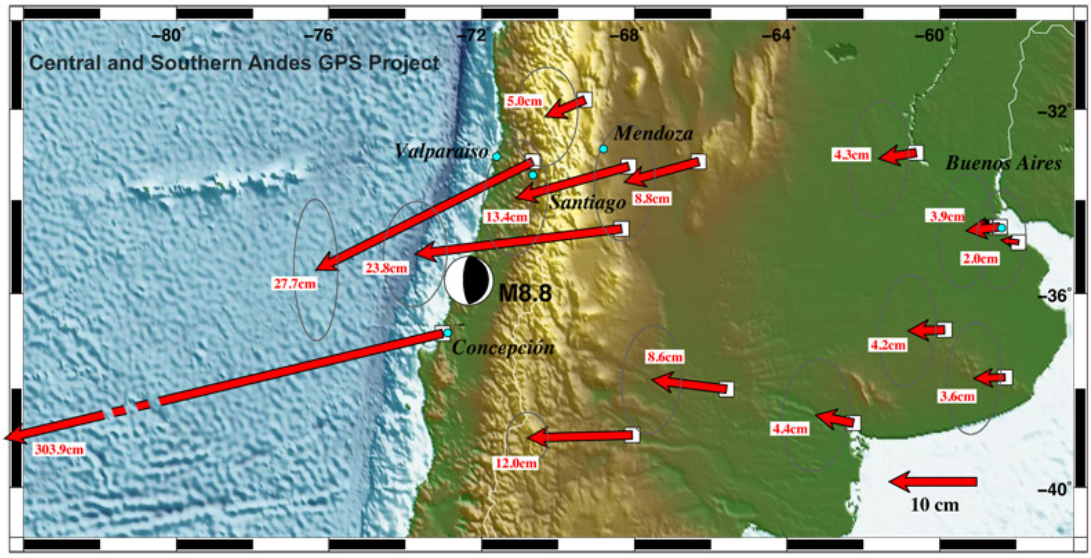

Fig. 3. Preliminary solution for the coseismic displacement field associated with the February 27, 2010 Maule earthquake in south-central Chile, based on GPS Geodetic measurements (as determined by James Foster and Ben Brooks of the University of Hawaii).

Due to the large extent of the epicentral region, the geologic conditions vary in the region from mountainous terrain and valleys to river and coastal terrains. Since the earthquake occurred towards the end of the southern hemisphere's summer season, the ground water conditions were favorably low. Thus, there were fewer landslides and ground related failures related to liquefaction, lateral spreading and bearing capacity. However, certain areas with soft soils were subjected to higher seismic energy focusing and ground motion amplification.

Closing of Seismic Gap - The region south of Valparaiso from about 34º to 36º South had been identified as a moderate seismic gap because it has not ruptured since1835 (Barrientos, 1987; Campos et al., 2002). The quake relieved stress by rupturing this seismic gap segment of the South American subduction zone, which separated the source regions of the great earthquakes of 1960 and 1906. However the area affected included portions of both the 1960 and 1906 events.

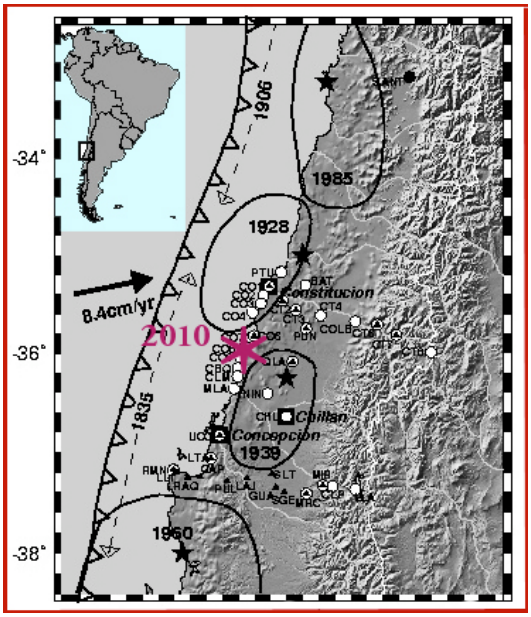

Fig. 4. Epicenter of the February 27, 2020 quake in relation to the 1960 and 1906 quakes. Seismic gap from about 34° South to 36° South (Modified web figure)

Planetary Impact – According to NASA, the 2010 earthquake resulted in a tiny shift in the Earth's axis estimated at three inches (8 cms), which affected the rate of its rotation, thus shortening the length of a day by 1.26 microseconds. It is believed that great earthquakes have a large enough moment to affect the earth's polar motion and that the impact is cumulative, not only on the Earth's axis of rotation and free nutation (due to non rigidity and spinning dynamics of the aspheric earth), but on the Chandler wobble (the Chandler Oscillation) of the earth's axis.

Additionally, great earthquakes such as that of 2010, are known to generate self-excited, long period, toroidal and spheroidal oscillations on the Earth's surface that tend to resonate over long periods of time, lasting many hours and days. The most important of the spheroidal oscillations have a fundamental mode estimated at 58 to 60 minutes. For example, the August 9, 1952 Kamchatka Earthquake had a fundamental frequency mode of 57 minutes (Benioff *et al.,* 1961). Similar frequency modes were determined for the May 1960 tsunami in Chile (Bogert, 1961; Ness *et al.,* 1961; Alsop *et al.,* 1961; Alsop, 1964b; Bolt, 1963; Connes *et al.,* 1962; Nowroozi and Alsop, 1968; and Dziewonski and Landisman, 1970), for the Kurile Islands earthquake of October 13, 1963 (Alsop, 1964a; Abe *et al.,* 1970; Dziewonski and Landisman, 1970), for the great earthquake of March Alaska, 1964 (Nowroozi, 1965; Smith, 1966; and Slichter, 1967), for the Rat Islands, February 4, 1965 (Nowroozi, 1966) and reported for the December 26, 2004 great Sumatra earthquake (Pararas-Carayannis, 2005).

Since spheroidal oscillations form standing waves with vertical excursion, these could contribute to tsunami-like sea level fluctuations along certain coastal areas. For example, 11 minutes after the earthquake in Chile there were oscillations of about 5 inches observed in Lake Pontchartrain, in Louisiana. However these were caused probably by the arrival of surface seismic waves rather than from Earth spheroidal oscillations. Slow crustal deformation and displacements associated with great earthquakes - such as the one in 1960 - can generate seismic waves with unusually long-periods (Kanamori & Cipar, 1974).

3. THE TSUNAMI

Based on the great magnitude of the February, 27, 2010 earthquake, its epicentral location and a confirmed initial tsunami height of 1.5m at a buoy near the source region (Talcahuano), a Pacific-wide tsunami warning was issued for Chile, Peru, Ecuador, Colombia, Antarctica, Panama, Costa Rica, Nicaragua, Pitcairn, Honduras, El Salvador, Guatemala, French Polynesia, Mexico, the Cook Islands, Kiribati, Kermadec Island, Niue, New Zealand, Tonga, American Samoa, Jarvis Island, Wallis-Futuna, Tokelau, Fiji, Australia, Palmyra Island, Johnston Island, Marshall Island, Midway Island, Wake Island, Tuvalu, Vanuatu, Howland-Baker, New Caledonia, Solomon Island, Nauru, Kosrae, Papua New Guinea, Pohnpei, Chuuk, Marcus Island, Indonesia, North Marianas, Guam, Yap, Belau, Philippines and Taiwan. Also, regional tsunami centers in the Pacific issued warnings. All tsunami warnings were canceled less than 18 hours later, except for those issued by Russia, Japan and the Philippines.

The tsunami damaged or destroyed many structures in Central Chile, including Constitución, Concepcion, Dichato and Pichilemu. There was a report of some damage to boats and a dock in San Diego, California and of flooding damage in northern Japan.

Tsunamigenic Area **-** A review of IRIS broadband data the earthquake aftershock distribution and of the moment tensor analysis of the February 27, 2010 earthquake indicate a general trend striking at 18^0 with a dip of $18^{0.}$ and a slip of almost 10 meters on the fault plane. The total rupture was about 550 km long, more than 100 km wide and extended to about 50 km in depth. Fig. 5 shows the approximate dimensions and orientation of the tsunamigenic area. It paralleled the coast of Chile and affected an area of about 82,500 square kms**.**

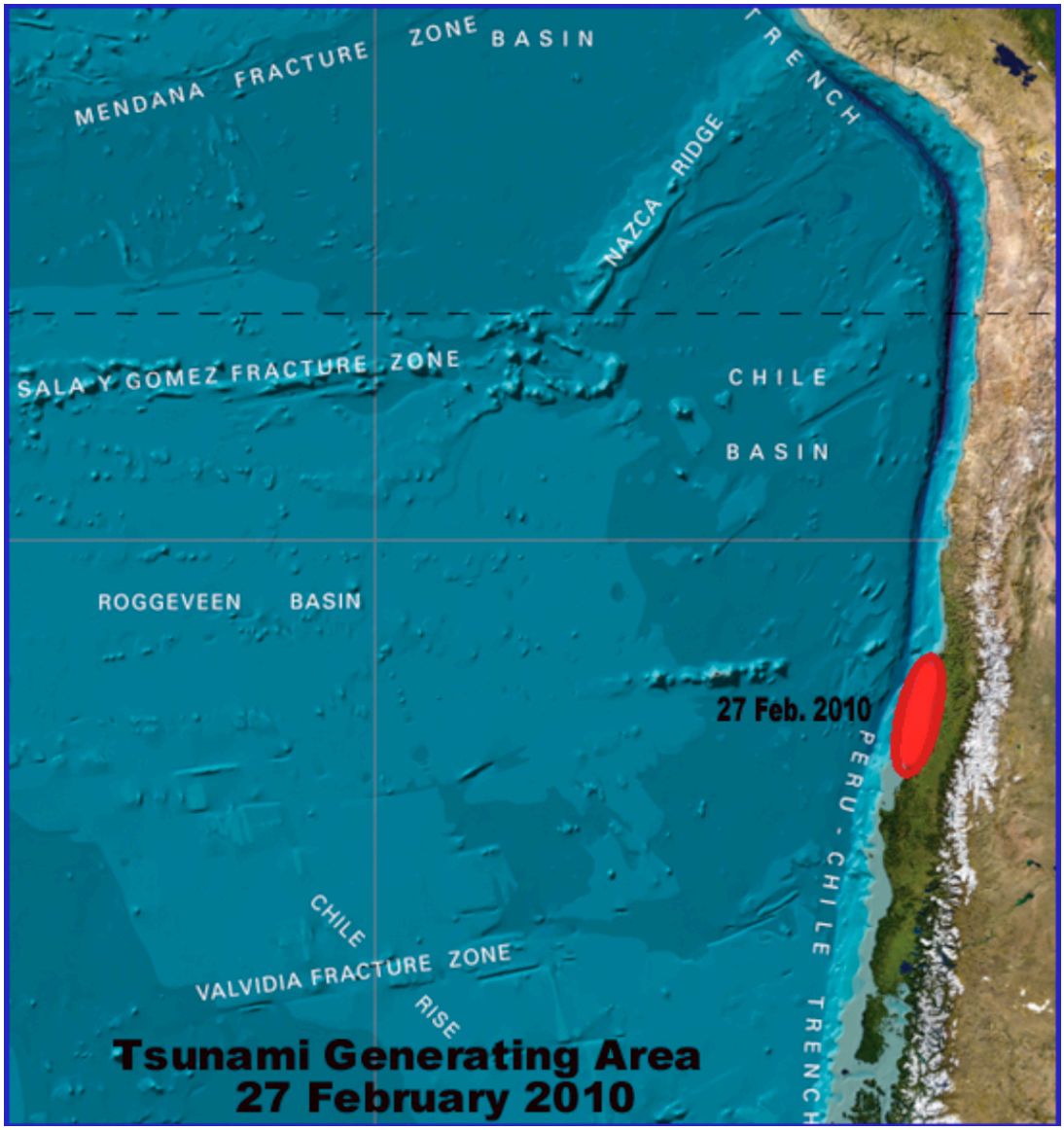

Fig. 5. Generating area of the February 27, 2010 tsunami based on earthquake aftershock distribution.

Ocean Floor Displacements and Initial Tsunami Height

The quake had a predominantly lateral strike slip with a smaller component of vertical dip slip motion. Crustal displacements were of a dipole nature (negative and positive) along a thrust fault approximately paralleling the Chilean coast in N18E orientation. There was a great deal of variation in the extent of vertical crustal displacements. Maximum displacements of up to 200 cms occurred in the offshore region north of Concepción. The maximum vertical uplifted portion (about 2 m) was on the continental side of the rift and the downward portion (about 1.8m) on the oceanic side of the rift. The 2 m uplift was the same as that of the 1835 earthquake, which was parallel to the strike of active faults and antiforms in the Arauco-Concepción region (Melnick et al., 2006). However, these represent maximum crustal displacement values diminishing away from the rift zone. In the region closer to Concepción the offshore vertical displacements were in the order of 50 cms. Upward, ground displacements must have also occurred on land along the affected coastal area - but these remain to be determined by geological surveys. The earthquake was very shallow in depth and this may have limited the extent of the tsunamigenic area.

The ocean area affected by such displacements, the tsunami generating area, is an approximate ellipse in which the fault occupies the major axis. Based on the above assumptions of vertical ocean floor displacements, the initial tsunami height in the generating area is estimated at a maximum of 1.5 - 1.78 meters above the undisturbed sea level.

3.1 Near-field Tsunami Effects

Shortly after the earthquake destructive tsunami waves struck the coastal areas of Central Chile. Coastal cities as Talcahuano, Coquimbo, Antofagasta and Caldera as well as the Juan Fernández Islands, were hardest hit. The largest wave was 9 feet near the quake's epicenter. North and south of the epicentral area at Valparaiso and at Coquimbo, the tsunami lost height rapidly. Overall, the death toll from the tsunami was relatively low in Chile as the waves arrived at night when most people were at home, away from the coastal areas.

Extensive tsunami reconnaissance conducted in the days following the earthquake by the USGS, the NSF funded Tsunami Ocean Sciences Group of the University of Southern California and of Georgia Tech, by EERI and many other groups. The survey findings have been extensively reported on the Internet. The survey by a USGS team determined that the tsunami caused substantial erosion and deposition, which caused local changes of almost 1 m in coastal elevations. The team found clear evidence at two open-coast sites that multiple waves arrived at different times and from different directions and that at an alluvial valley the tsunami inundation was as much as 2.35 km inland. The tsunami run-up heights along the open coast were higher thus differing from those recorded by tide gauges.

Curanipe – Curanipe - that was only 8 km (5 mi) from the epicenter – as well as Pichilemu, Cobquecura, Cauquenes and Parral were hit hard by the tsunami.

Talcahuano **-** A tsunami struck the port city, which is part of greater Concepción. The greatest impact was along Bahia Concepción and Rio Andalien. The first wave arrived

about 19 minutes after the earthquake. Maximum-recorded wave was 2.34 m (7.7 ft) high. The tsunami was very damaging at the port where large boats and shipping containers were carried inland and piled upon one another. The waves damaged buildings, knocked down trees and blanketed the coastal area with extensive deposits of mud. There were unconfirmed reports of a 15-m-high wave at a beach along the Tumbes Peninsula.

Dichato **-** A total of seven waves were observed, the sixth being the largest and most damaging. Maximum, reported tsunami wave height was 10 meters and 90% of the town was destroyed. About 50 people were missing and presumed dead. Maximum reported inundation was 2.2 km into a valley.

Constitución **-** Both the earthquake and subsequent tsunami caused damage at Pelluhue and Constitución. A wave estimated as much as 2m high swept about five blocks into the city about 30 minutes after quake. As many as 350 people are believed to have to have died from the combined effects of the earthquake and the tsunami and hundreds more were reported as missing.

Lioca **-** Tsunami waves swamped the coastal village of Lloca.

Valparaiso **-** A 1.29 meter tsunami was observed 20 minutes after the main earthquake at Valparaiso, to the north of the epicentral area. Maximum-recorded height was 2.61 meters 261 at Valparaiso,

Coquimbo **-** A maximum of 1.64-meter tsunami was recorded at Coquimbo, to the south of the epicentral area.

San Juan Bautista, Juan Fernández Islands **-** Destructive waves struck the sparsely populated volcanic island group located about 667 km (360 nautical miles; 414 miles) off the coast of Central Chile. The Juan Fernández Archipelago consists of three islands: Robinson Crusoe, Alejandro Selkirk and the small Santa Clara. According to local reports, most of the tsunami fatalities and losses occurred on Robinson Crusoe Island, the largest of the group. There were unconfirmed reports that a gigantic 40-meter (130 feet) high wave hit Robinson Crusoe Island (Spinali, 2010; Newsolio, 2010). However, later reports indicated that tsunami waves of up to 3 m (10 ft) swept into Cumberland Bay and inundated almost 2 miles into the town of San Juan Bautista, the capital. The waves destroyed the local inn, homes along the water, the school, municipal offices, fishermen's shacks, shops, and a church. According to local reports, fifteen people died and twenty-two more were missing.

3.2 Far-field Tsunami Effects

Hawaiian Islands **-** Waves of up to 5 ft were reported in Kahului, Maui, and in Hilo about 15 hours after the earthquake, but did little damage.

California **-** The tsunami was up to 0.53 m in height high and reportedly did some damage. Navigational buoys in Ventura County, California, sustained minor damage as a result of a 2-foot surge and waves, according to the Alaska Tsunami Warning Center. The Ventura

County Fire Department had one report of damage to a resident's dock from the surge. Minor damage occurred in San Diego.

Mexico **-** In Acapulco the recorded tsunami height in was 0.62 m.

French Polynesia **-** At the Marquesas Islands, the tsunami measured at 1.79 m (5 ft), but apparently did little damage.

Tonga **-** Up to 50,000 people evacuated inland in anticipation of the tsunami. There were report of a wave of up to 6.5 feet hitting a small northern island, but no damage occurred.

New Zealand and Australia **-** Tide gauges recorded a rise of up to 15 cm only.

Japan **-** Based on experience from the destructive 1960 tsunami which resulted in many deaths, waves of at least 9 ft. in height had been predicted for northern Hokkaido Thousands of people were evacuated from low-lying coastal areas in anticipation of a destructive tsunami. The waves that reached Japan's harbors 24 hours after the quake, raised the water level by up to 0.82 m. Extensive localized flooding occurred in Kesennuma and in Shichigahama, Miyagi Prefecture (state), in northern Japan. At the Tōhoku region damage to the fisheries business was estimated at US $66.7 million.

4. ANALYSIS AND EVALUATION OF THE FEBRUARY 27, 2010 TSUNAMI

The tsunami of February 27, 2010 was generated from an earthquake in the same active seismotectonic zone as that of May 22, 1960 – the latter being extremely destructive, not only locally in Chile but throughout the Pacific Ocean Basin. Given the 2010 earthquake's great magnitude, shallow focal depth and coastal location, it was expected that the far field tsunami impact would have been somewhat similar to that of 1960. However, it was not as severe as anticipated. The following is a cursory review and evaluation of the tsunami generating source characteristics, of the near-field impact and of the possible reasons for the diminished far-field effects. Specifically, the present study examines structural anomalies in the geometry of subduction along Chile's central seismic zone and of source characteristics of past tsunamigenic earthquakes along this segment of the subduction zone. Furthermore, it provides a comparison of similarities and differences of the 2010 event with those which occurred in 1960 and in 1575 - in terms of focal mechanisms, extent of ground and ocean floor displacements, aftershock hypocenter space/time distribution, subduction geometry, absorption, tsunamigenic efficiency, tsunami energy trapping and ducting, as well as of tsunami heights recorded by tide gauge stations.

4.1 Chile's Central Zone Seismicity and Potential for Tsunamigenic Earthquakes.

The Peru-Chile Trench - also known as the Atacama Trench - is the active boundary of collision of the Nazca Plate with the South American Plate. Subduction of the Nazca plate beneath the South America continent is not homogeneous. As a result, asperities and structural complications have caused segmentation along the entire margin, resulting in zones with different rates of slip, seismic activity, volcanism, uplift, terracing and orogenic

processes. Different sections of the margin are segmented by great fractures. Each segment along the Great Peru-Chile Trench has its own characteristic parameters of collision and structural geometry and thus, different potential for large earthquakes and destructive tsunamis. Based on seismicity patterns and clustering of events, Chile can be divided into three distinct seismic regions.

Along central Chile, active tectonic convergence results in extreme seismicity and crustal deformation. The extensive central zone is of particular interest because of its a long history of great subduction zone earthquakes of magnitude 8 or larger that have generated destructive tsunamis. The central zone extends from 33ºS to 41ºS and this too can be divided into segments that have their own distinct tectonic characteristics, depending on the geometry of subduction, angle of dip and local anomalies. Compressional, tensional and large thrust seismic events have occurred along the entire central zone. Only the large thrust earthquakes are capable of generating significant tsunamis. The following are the distinct segments of Chile's central seismic zone and historic records of tsunami activity.

1. The northern end of the central seismic zone from 33º-34ºS is delineated by the oblique subduction of the leading edge of the Juan Fernández ridge with the Peru-Chile Trench near Valparaiso and the appearance of volcanism at the southern end. Five tsunamigenic earthquakes have occurred in this area in historic times: November 19, 1811; November 19, 1822; October 16, 1868; August 17, 1906 and March 3, 1985.

   The collision of the ridge plays an important role in the development of the forearc features in this region, in the landward deflection of the Peru-Chile trench axis and in the crustal deformation of the convergent margin. For example, a major (*M*w 6.7), outer-rise earthquake with a tensional focal mechanism and an unusually high, clustered aftershock sequence occurred on April 9, 2001 (Fromm et al., 2006), supports the existence of preexisting fractures along the ridge that extend to the mainland. Outer rise, compressional and tensional seismicity and ridge collision can be expected to induce uplift of the leading edge of the overriding plate, steepen the inner wall of the trench, compress the sediments along the accretionary wedge and result in additional deformations (McCann & Habermann, 1989). Ridge collision and outer rise events can also nucleate thrust faulting by acting as conduits to hydrate the subducting slab and generate events such as that of 1906 in the vicinity of Valparaiso, or the 1960 at the southern end of the central zone, near Valdivia. However, earthquakes in this northern part of the central seismic zone can be expected to generate local destructive tsunamis, but it is very unlikely that these would have a significant far-field impact in the Pacific basin.

2. South of Valparaiso from 34º-36ºS, a seismic gap existed (Barrientos, 1987). This is the segment that was ruptured by the February 27, 2010 earthquake. Four earthquakes with magnitudes of 7.5 or larger have occurred previously.

3. The Concepcion Region extends from 36º to 37ºS. This region generated two large earthquakes in 1835 and 1939 with magnitudes greater than 8.0. The 1835 quake generated a destructive tsunami. Lesser magnitude earthquakes occurred in 1751, 1868, 1878, 1953 and 1971.

4. The forearc of the active convergent margin of south-central Chile from 37º to 41ºS is

located within the rupture zone of the 1960 Chile earthquake and is characterized by distinct structural changes caused by the geometry of subduction (Rehak et al., 2008). This southern region generated large earthquakes, on October 28, 1562; February 8,1570; December 16, 1575, March 15, 1657, and May 22, 1960. Of these, the 1562, the 1570, the 1575, and the 1960 earthquakes generated destructive tsunamis, locally and in the Pacific Basin.

4.2 Historic Tsunamis of Chile's Central Seismic Zone

The historic record of earthquakes and tsunamis in Chile begins with the arrival of the Spaniards in 1541. The record shows that at least thirty-five tsunamis were generated along the entire subduction zone of Chile by earthquakes of different magnitudes. The first documented tsunamigenic quake occurred near Concepción in 1562 (Iida et al., 1967; Pararas-Carayannis, 1968; Pararas-Carayannis & Calebaugh, 1977) Since then, earthquakes generated tsunamis of various intensities along Chile's coastlines. Great earthquakes along Chile's northern region in 1586, 1687, 1868, and 1877 generated tsunamis that had far-field impact in the Pacific. Seventeen significant tsunamis had their origin along Chile's central seismic zone. Specifically, three tsunamis were generated near the Coquimbo region in 1849, 1943 and 1955. Four more were generated in the Valparaiso region in 1730, 1822, 1871 and 1906. One tsunami originated in the Maule region in 1928. Five more tsunamis originated in the Bio-Bio region in 1562, 1570, 1657, 1751 and 1835. Finally, four more occurred in the Los Lagos region in 1575, 1737, 1837 and 1960. Since 1973, there have been thirteen earthquakes with M>7 along Chile's central seismic zone. The following events generated the more destructive tsunamis in the region.

October 28, 1562 **-** Great earthquake (Mw8) with epicenter at 38.0 S, 73.5 W. generated a destructive tsunami, which reached a maximum height of up to 16 meters near Concepción.

February 8, 1570 **-** Great earthquake with estimated magnitude Mw8.8 and epicenter at 37.0 S, 73.0, W. generated tsunami with maximum height of 4 meters.

December 16, 1575 **-** Extremely severe, great earthquake (similar to 1960) had its epicenter at about 40.0 S., 70.0 W. Strong aftershocks lasted for forty days. There was destruction of five Indian territories south of the Bio-Bio River (Imperial, Valdivia, Villarrica, Osorno and Castro). The quake generated very destructive tsunami waves, which reached Valdivia, 25 km up the river by the same name, destroying houses, uprooting trees and sinking two galleons at the port. Along the coast of La Imperial, north of Valdivia, the tsunami killed 100 people. Landslides blocked the river. A subsequent break of a dam killed 1200 more.

March 15, 1657 - A great earthquake (estimated Mw8.0) and epicenter at about 37.0 S., 73.0 W. generated a tsunami with maximum height of 8.0 meters.

1730 **-** An earthquake near Valparaíso generated a tsunami, which caused flooding, and damage in Japan.

1751 **-** Great earthquake (Mw8) near Concepción (36.5S. 74.0W) generated destructive tsunami.

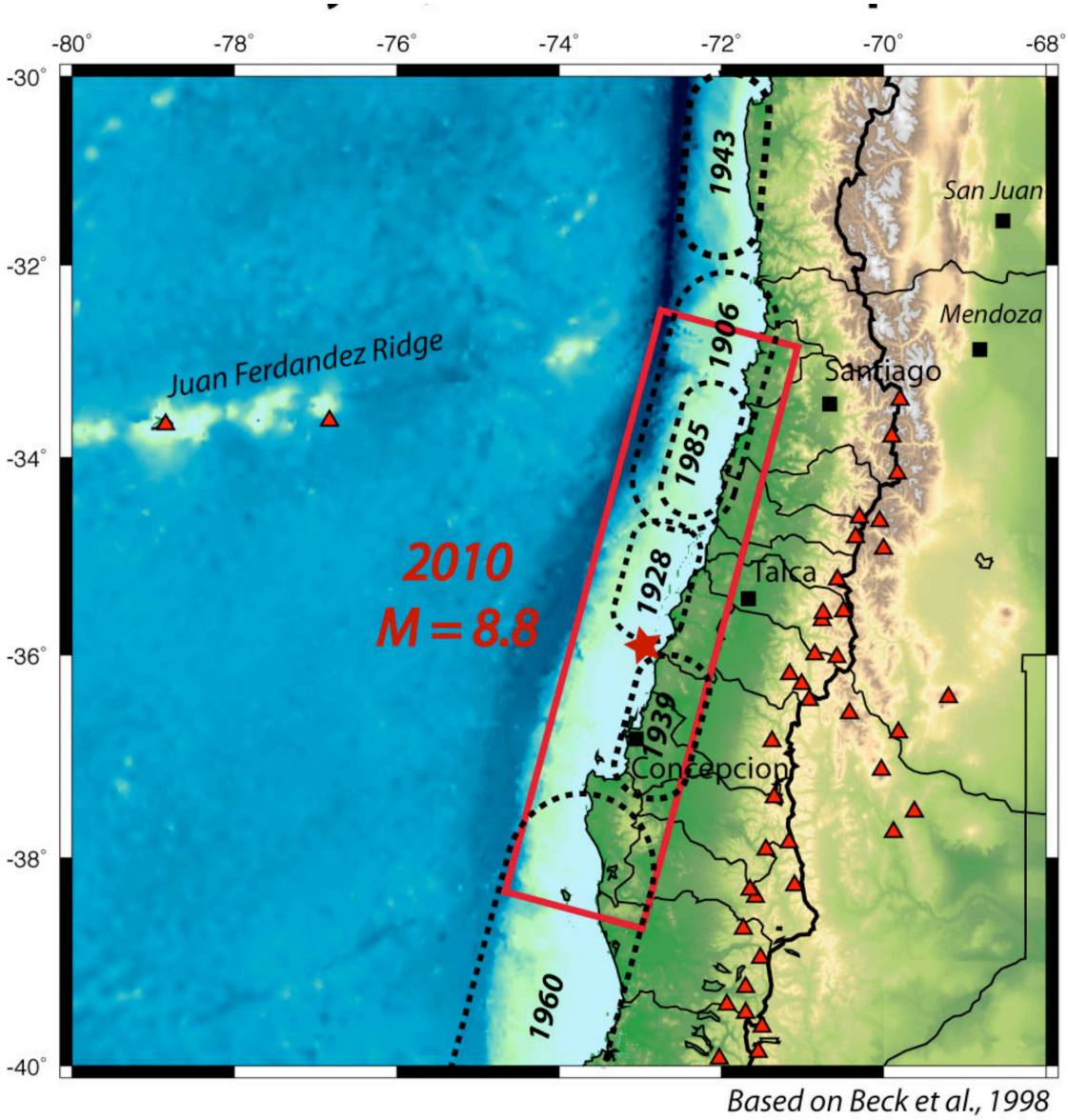

Fig. 6. Area affected by the February 27, 2010 earthquake in relation to historic earthquakes and tsunamis along Chile's central seismic zone. Overlap with the 1960, 1928, 1985 and 1906 events (modified after Beck et al., 1998).

Nov. 19, 1822 - A great earthquake with estimated magnitude Mw8.5 and epicenter at about 33.0S. 71.4W. generated destructive tsunami of 3.5 meters.

February 20, 1835 - Great earthquake (Mw8.2) with epicenter at 36.8S, 73.0W. generated destructive tsunami.

August 17, 1906 - A great earthquake (Mw8.6) with epicenter at 33.0 S., 72.0 W. generated a Pacific-wide destructive tsunami. In Hawaii, waves of 3.5 meters caused damage.

November 27, 1922 **-** Great earthquake (Mw8.5) with epicenter north of Valparaiso generated a destructive tsunami that significantly impacted central Chile, killing several hundred people and causing severe property damage. A 9-meter local tsunami was particularly damaging near the town of Coquimbo. The tsunami crossed the Pacific and impacted Hawaii, washing away boats in Hilo harbor, Hawaii.

May 22, 1960 **-** This was the largest earthquake in recorded history and occurred about 240 nautical miles to the SSW of the February 27, 2010 quake. Its magnitude was Mw9.5. It was extremely destructive and very similar to the December 16, 1575 event in same region. Its rupture was estimated to be more than 1,000 kms. The Pacific-wide tsunami that was generated caused extremely devastation in Chile, Hawaii, California, Pitcairn Island, New Guinea, New Zealand, Japan, Okinawa, Philippines and as far away as Australia (4.5m). In Chile, the 1960 quake/tsunami killed 1,655 people and left 2 million people home less. The tsunami accounted for around 200 fatalities in Chile, 61 in Hawaii, 32 in the Philippines, and another 138 in Japan.

4.3 Pre-existing Seismic Gap and Subsequent Stress Release

There are narrow belts of high seismic activity with characteristic clustering of earthquakes near the surface along Chile's entire seismic zone. These are indicative of anomalies that can influence tsunamigenic efficiency. Also, intermediate-depth earthquakes tend to cluster in space. For example, there is a known gap in activity between focal depths of 320 and 525 kms, between latitudes 25.5º and 27ºS. This particular northern region has generated many large shallow earthquakes. The deeper earthquakes are indicative of complex interaction of tectonic plates and anomalies, which can account for differences in the spatial distribution and clustering of the shallower events, as well as for seismic gaps where future large tsunamigenic earthquakes could strike. The same type of shallow and deep hypocenter clustering occurs further south.

The 2010 earthquake involved thrust faulting in the coastal segment of Chile's central seismic zone, where similar anomalies are evident. As mentioned, the region south of Valparaiso from about 34º to 36º South had been identified as a moderate seismic gap where no great earthquake had occurred for many years. With the exception of a 1939 earthquake - inland and deeper - there had been no major or great earthquake in this area for about 120 years. This segment was highly stressed because of the active and oblique subduction of Nazca tectonic plate below South America at high rate of 6.8 cms/yr. The February 27, 2010 earthquake closed the gap.

4.4 Examination of the Rupture Process

Earthquakes along the entire shallow South American subduction zone exhibit heterogeneous and complex rupture characteristics that can be linked to certain Nazca Plate features and subduction zone structure (Bilek, 2009). The February 27, 2010 quake had such a complicated rupture process, which must be examined to help understand the generation of tsunamis from Chile's central seismic zone from about 33º to 37ºS.

The length of the total rupture of the earthquake was about 550 km long and extended to about 50 km in depth. It affected an area of about 82,500 square kms. The

rupture connected directly to that of the great (M=9.5) 1960 tsunamigenic earthquake, which had its origin near Valdivia, immediately to the south. The largest amounts of the 2010 quake's rupture occurred in the first 60 seconds, but smaller displacements continued for up to 200 seconds. A preliminary review of seismic waves radiated by the quake and the distribution and clustering of aftershocks in the following three days, as observed by the GEOFON-measuring network of the GFZ up to March 3, 2010, indicated that the rupture was not continuous. During the first 134 seconds after the start of the rupture and during the first minute, only the immediate region around the actual epicenter appeared to be active. In the second minute the zone of activity moved north towards Santiago. After that the region south of Concepción became active for a short time.

The anomalous rupture process of this earthquake is indicative of complexity in moment release and in slip distribution that can be related to structural variations within the subducting and the overriding plates. It is also significant in understanding how the tsunami's source mechanism is affected by such anomalous process and whether it can be related to the less intense far-field effects of the tsunami.

Also, the numerous strong aftershocks that followed the main shock - some over M6 in magnitude – occurred over a large area. The unusual clustering and chronological sequencing of these aftershocks, as discussed in the next section, are indicative of a segmented and gradual release of tectonic stress. Segmented ruptures and gradual release of energy result in sea floor displacements that will affect significantly tsunamigenic efficiency and near and far-field tsunami impacts. For example, the September 12, 2007 event off Sumatra involved two successive earthquakes, numerous aftershocks and a later strong shock further south/southeast within the same segment that was ruptured by a single great earthquake (Mw=8.7) in 1833 - which generated a very destructive tsunami. However the two Sumatra earthquakes in 2007 which occurred in sequence, released the tectonic stress gradually, thus contributing to the relatively smaller tsunami that was observed in Padang and elsewhere (Pararas-Carayannis, 2007). The unusual rupturing process of the 2010 earthquake also released energy gradually, which could partially account for the less severe near and far-field tsunami effects.

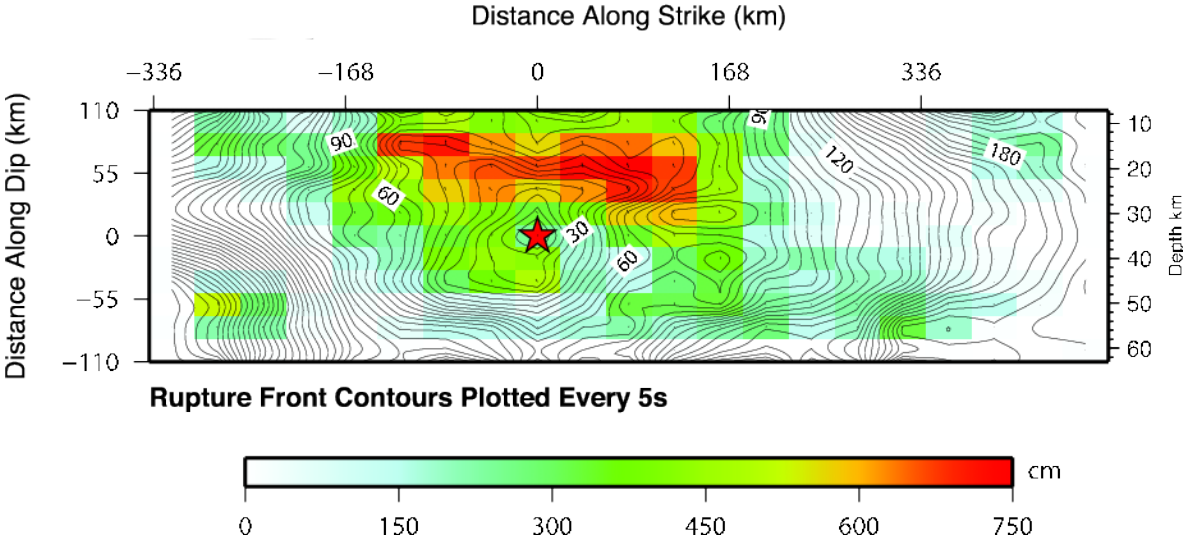

Fig. 7. Rupture process of the February 27, 2010 Earthquake (NEIS)

4.5. Examination of Aftershock Hypocenter Spatial Distribution and Focal Mechanisms

A tsunami's generating area can be determined from the distribution of aftershocks over a coastal area and offshore following a large earthquake, as the aftershocks usually indicate gravitational adjustments of crustal material that contributed to tsunami generation.

As previously stated, there was a vigorous aftershock sequence following the main February 27, 2010 shock. The range of aftershocks over the next days and weeks extended from 33.062^0- 38.584**0** South and from 71.574^0 -75.199^0 West. There was an unusual clustering in the spatial distribution of the aftershocks in the first few minutes. The initial aftershock sequence indicated the anomalous rupture associated with the earthquake - which must be examined as it may provide clues as to tsunami generation mechanisms in this Central Region of Chile. Furthermore, the swarms, which occurred near the Libertador O'Higgins and Bio-Bio regions following the main shock, appear to have acted as independent families of sequential seismic events. However, it should be pointed out that it is not uncommon for this region to experience clusters of earthquakes which may be perceived as aftershocks, but which in fact may be separate events on adjacent faults, triggered by stress transference.

Application of statistical procedures - such as clustering of groupings and pruning of outlying events – indicated that three major clusters of "aftershocks" occurred, as well as about a dozen small clusters of independent families of seismic events (personal communication with P. Zhol). Whether all of these were really aftershocks or separate events triggered by stress transference, remains to be investigated. Energy may have been released gradually by separate events – as with the September 12, 2007 event off Sumatra (Pararas-Carayannis, 2007) – which may partially account for the lesser far-field impact of the 2010 Chilean tsunami.

The spatial distribution of aftershock hypocenters and their chronological sequence were examined in trying to understand the tsunami's source mechanism as well as the directivity of its energy flux propagation. Review of focal mechanisms and of aftershocks can help understand the type of sea floor displacements that occurred that contributed to tsunami generation and whether the recorded swarms involved normal faulting - which would indicate simple aftershock gravitational settling - or thrust faulting, which would indicate separate events on adjacent faults caused by compression and stress transference.

Also, the problem of spatial distribution and clustering of aftershocks can be studied mathematically as a topological, geometrical manifold for which time is an important dimension, in the sense that each new seismic event (alleged as aftershock) must be considered in terms of previous history and whether it is a member of any existing clusters. What is even more important in understanding the tsunami source mechanism associated with a great earthquake such as the 2010, is the type of crustal displacements and the spatial properties each subsequent seismic event involved, relative to the initial rupture and to subsequent failures on adjacent faults. In other words, how stress is passed-on spatially from one event to another before it is totally released. However, such considerations require a more detailed analysis of geometrical topology and are outside the scope of the present study at this time.

Sequence of Aftershocks and Independent Earthquakes: The following sequence of events took place. An aftershock of M6.2 was recorded 20 minutes after the initial quake. Two more aftershocks with magnitudes M5.4 and M5.6 followed within an hour. An M6.9-magnitude offshore earthquake struck approximately 300 kilometers southwest less than 90 minutes after the initial shock; however, this may have been a separate event that may not have been related to the main shock. In the 2 1/2 hours following the 90-second main shock, 11 more were recorded. Up to the 1st of March a total of 121 aftershocks with magnitude 5.0 or greater were recorded (USGS, NEIC). Eight of these had magnitudes of 6.0 or greater. There was an apparent clustering in the distribution of these aftershocks (Fig. 8 which can be correlated to the anomalous rupture process and perhaps to the tsunami generation mechanism in the sense that displacements of the ocean floor occurred along different faults.

Fig. 8. Initial aftershock distribution showing four distinct clusters, one near the earthquake epicenter, another one closer to Santiago, a third one near Concepción and a fourth one to the south.

On March 5, two more aftershocks above M6.0 were reported. The first was a M6.3, off the coast of Bio-Bio region. The second was a M6.6 near the epicenter of the original quake. On March 11, a M6.9 quake occurred near Pichilemu in the Libertador O'Higgins Region. It was reported as an aftershock – but apparently it was an independent event. It was followed by two aftershocks of M6.7 and M6.0. However, it will suffice to say that two remarkable events occurred on March 11 but 16 minutes apart, near Libertador O'Higgins which could not be considered as aftershocks, given their magnitude and depth (Table 1).

Table 1. Independent Seismic Events

Date	Time (UTC)	Latitude	Longitude	Magnitude	Depth
11 March	14:55	34.287 S	71.657 W	6.9	44
11 March	14:39	34.290 S	71.950 W	7.2	35

On March 15, two aftershocks of the main February 2010 earthquake were reported, one was a shallow (18 kms) event of M6.1 offshore Maule and the other a M6.7 offshore the Bio-Bio Region, near Cobquecura. Two more minor aftershocks of M5.5 followed.

On March 17, an M5.2 earthquake occurred in Aisén, in Southern Chile. On March 18 an M5.2 earthquake occurred in Los Lagos. On March 26, an M6.2 earthquake occurred in the Atacama Desert region, in Northern Chile.

By March 29, 2010, a total 458 aftershocks had been recorded.

The Bio-Bio region had an unusual sequence of aftershocks and what appear to be independent quakes. A strong M5.9 aftershock struck on April 2. Its epicenter was on land and its focal depth was 39 km. Another strong M6.2 aftershock struck again the same region on April 23. On May 3, a shallow (20Km) M6.4 earthquake struck again the offshore Bio-Bio region. On July 14, 2010, another M6.5 earthquake occurred again in the same area. The significance of the aftershock distribution and of their spatial clustering for tsunami generation is discussed in a subsequent section.

4.6 Source Mechanism of the February 27, 2010 Earthquake and Tsunami

Based on the areal extent and clustering of aftershocks and on geological and macroseismic observations, we can conclude that the earthquake of February 27, 2010 involved multiple ruptures of adjacent faults and various vertical crustal displacements of the ocean floor. Although the overall affected area was extensive, the greater vertical ocean floor displacements of up to 2 meters occurred in the region north of Concepción while the rest of the tsunami source area had displacements of 50 centimeters. The bulk of the earthquake energy that went into tsunami generation was in that limited region, thus the near and far-field effects were not as severe as those of the 1960 event that involved greater ocean floor displacements over a very extensive area. Furthermore most of the tsunami's energy was directed towards Talcahuano but also towards the Juan Fernández islands and French Polynesia. As discussed subsequently, the Juan Fernández ridge and the O'Higgins seamount further altered the far-field characteristics of the tsunami.

4.7 Examination of a Reported 40-meter Tsunami Wave

Shortly after the earthquake, there was an unconfirmed report that a 40-meter high tsunami wave swept over San Juan Bautista on Robinson Crusoe island of the Juan Fernández Archipelago (Spinali, 2010; Newsolio, 2010). The report was clearly erroneous as such wave was physically impossible. The small town is at Cumberland Bay on the northern center of the

mountainous coast of the island and the bay has a northeast configuration (Fig. 9). The tsunami generating area was some 670 km away to the southeast. Thus, the actual destruction at San Juan Bautista resulted from a 3 m (10 ft) tsunami, which resulted from edge waves that refracted around the north part of the island and perhaps were amplified by Cumberland Bay's bathymetry.

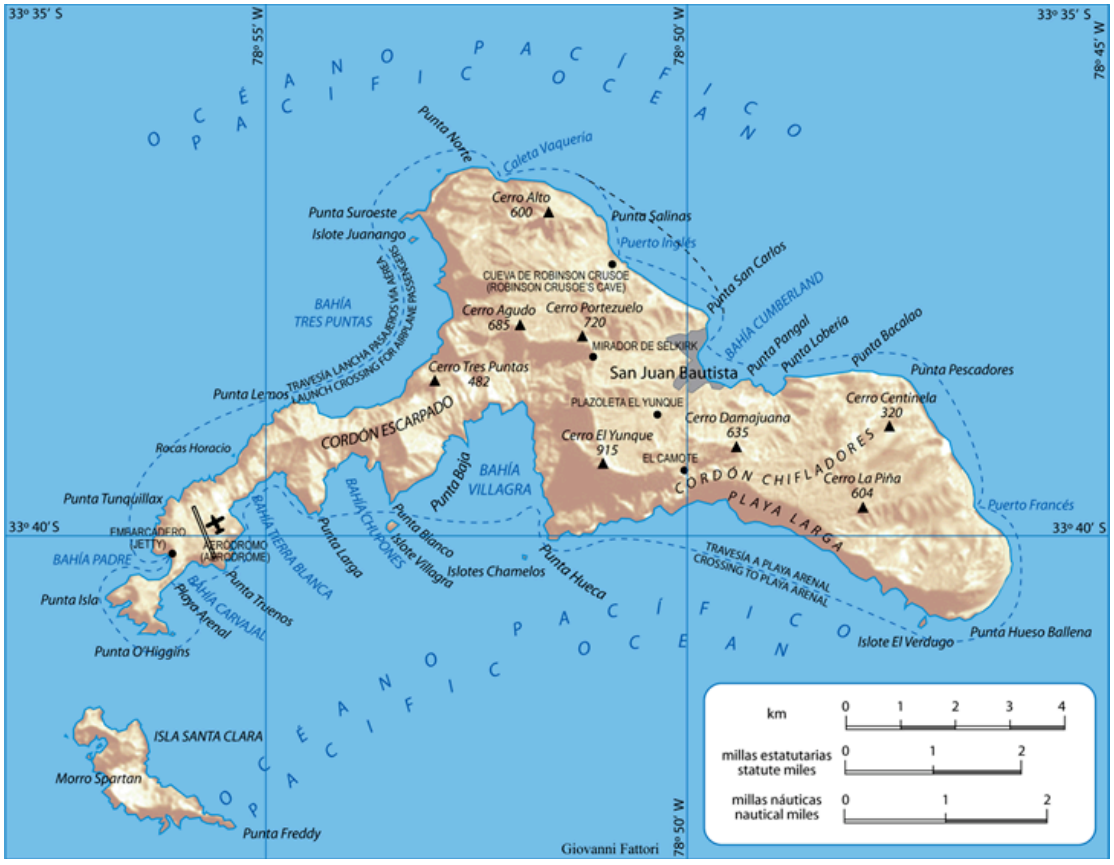

Fig. 9. Robinson Crusoe Island of the Juan Fernández Archipelago. Tsunami destruction occurred in the town San Juan Bautista in Cumberland Bay on the north shore.

Although the reported 40-meter wave at San Juan Bautista was a gross exaggeration, it may not be outside the realm of possibility for some other coastal location on the island. As demonstrated for the November 26, 2006 Kuril islands tsunami at Crescent City, both local and distant bathymetric features and local resonance can be changed by natural shelf oscillations (eigenmodes) which can amplify local tsunami height, change tsunami travel time and alter characteristics of refraction and reflection and the trapping mechanism of tsunami wave energy (Horillo et al., 2007).

Much larger tsunami waves than those observed at San Juan Bautista probably struck the southern uninhabited coasts of the islands. The combination of bathymetric features and near shore resonance probably contributed to larger waves - which may have occurred on the low-lying, south coast of (i.e. Playa Larga on Robinson Crusoe island) or at "Isla Afuera" at the western end of the Juan Fernández Archipelago.

4.8 Tsunami Energy Trapping and Ducting by the Juan Fernández Submarine Ridge and Other Bathymetric Features.

Tsunami properties are related to such characteristics as extent of ocean floor displacements and directional orientation of source. Trapping of tsunami energy can be induced by the submarine bathymetry of a sea basin bounded by islands and by seamounts. Excitation of "trapped" eigenmodes (free oscillations) of a basin may increase substantially tsunami height (Tinti & Vannini, 1995), but such resonance effect would be expected to enhance tsunami run-up locally. However, energy trapping by ridges and seamounts can also contribute to directional ducting and the refocusing of tsunami energy directivity over great distances.

Being in the direct path of the February 27, 2010 tsunami, prominent bathymetric features such as the Juan Fernández submarine ridge and the O' Higgins seamount, probably contributed to energy trapping and ducting of tsunami energy flux propagation. Further trapping and ducting probably occurred along the Nazca ridge to the north. Such concentrated energy trapping and ducting of long period waves appears to occur when a tsunami propagates for large distances over oceanic ridges. This was demonstrated by the non-linear, shallow water (NLSW) numerical simulation study of spatial derivatives of global propagation of the tsunami of 26 December 2004 (Kowalik et al. 2005). The high spatial resolution (one minute grid) modeling study of the 2004 tsunami on a supercomputer (with close to 200 million grid points) indicated that very small numerical dispersion occurs when tsunamis waves travel over long distances - and that the Coriolis force plays only a secondary role in the trapping.

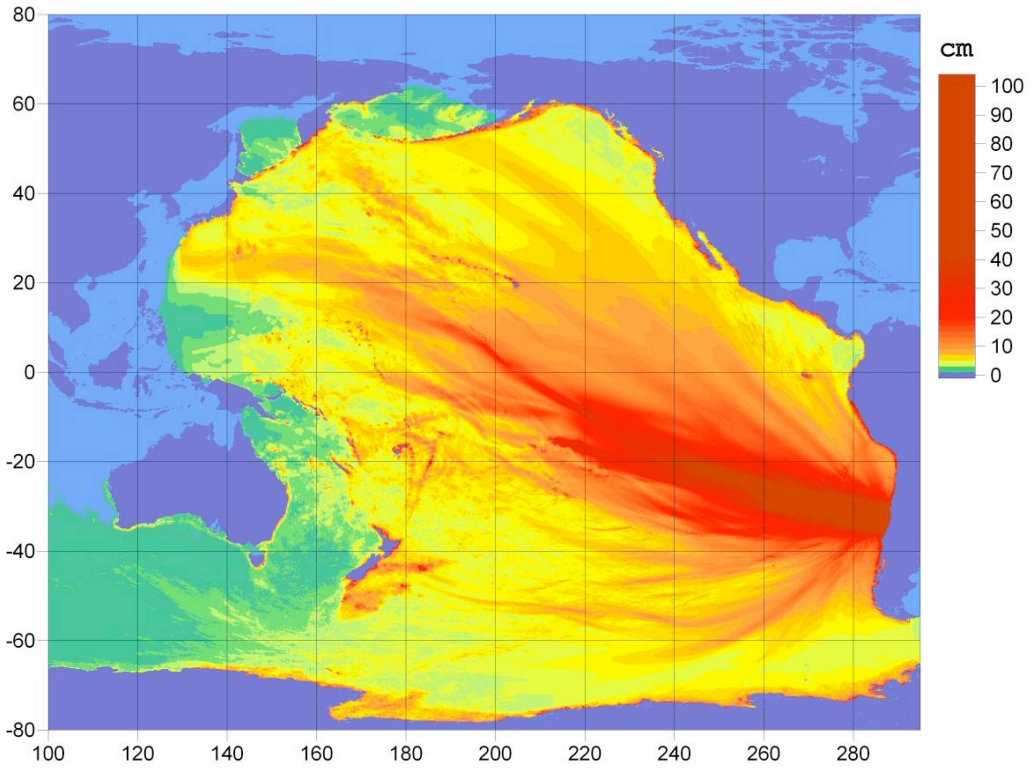

Fig. 10. NOAA map showing predicted amplitudes of the February 27, 2010 tsunami.

Although of lesser spatial grid resolution, the NOAA height forecast model of the 2010 tsunami (Fig. 10), shows bands of stronger energy flux signal in the direction of French Polynesia and towards the north and lesser energy flux directivity towards Hawaii, Japan, New Zealand and Australia. The higher recording of the tsunami in the Marquesas Islands supports such selective directivity in the propagation of tsunami energy towards French Polynesia, which in turn suggests that energy trapping and ducting by the Juan Fernández Submarine Ridge may have been a factor. In the same forecast model, there is a relatively stronger signal directed towards the north Pacific, which indicates some directional amplification, perhaps due to trapping and ducting by some other submarine feature in the immediate vicinity – which may account for the higher tsunami recording in Valparaiso - or the Nazca Ridge further north.

5. COMPARISON OF THE 27 FEBRUARY 2010 AND 22 MAY 1960 EARTHQUAKES AND TSUNAMIS

The February 27, 2010 earthquake generated a tsunami that was destructive locally but was relatively harmless in the rest of the Pacific. By contrast, the May 22, 1960 Chilean earthquake generated tsunami waves of up to 10 meters throughout the Pacific Basin, which devastated Hilo, Hawaii and caused damage as far away as Japan and New Zealand. Comparing similarities and differences between these two events can help understand the seismotectonic characteristics of Chile's central seismic zone from 33ºS to 41ºS and its potential for large earthquakes that can generate tsunamis with significant far-field impacts. Indeed the two events had differences in source characteristics, energy release, geometry of subduction, angle of dip and extent of crustal displacements on land and in the ocean. Also, there were significant differences in coastal geomorphology, spatial distribution of hypocenters, clustering and time sequence of aftershocks and of seismic gaps at depth.

5.1 Differences in Source Characteristics

Both the 2010 and the 1960 earthquakes – as well as that of 1545 - occurred on different segments of Chile's central seismic zone but were caused by the same, on-going crustal deformation associated with oblique tectonic convergence and ridge collision that results in accumulation of strain along this region.

A large precursor event occurred before the great 1960 earthquake struck, but this was not the case not with the 2010 quake. Also, the 1960 quake was associated with much larger subsidence and uplift. Specifically, on 21 May 1960 a great precursor quake with epicenter in the zone of Concepción caused extensive damage to towns in the area and generated a small tsunami, which recorded at 20 to 30 cm in height by the Valparaiso tide gauge. A few hours later, at about 1510 hours on 22 May 1960, the great earthquake struck. With epicenter in the province of Llanquihue, it caused extensive destruction in the region between Concepción and Chiloe and was particularly damaging at Puerto Montt, Valdivia, Ancud, Castro, and Corral. The quake caused both subsidence and uplift of land on Chile's coasts and offshore islands. Isla Guafo for example rose by 3 to 4 meters.

Epicenters **-** The epicenter of the 2010 earthquake was at 35.909 S., 72.733 W offshore from Maule. The epicenter the 1960 earthquake was at 39.50 S., 74.30 W. off the coast of the Valdivia province.

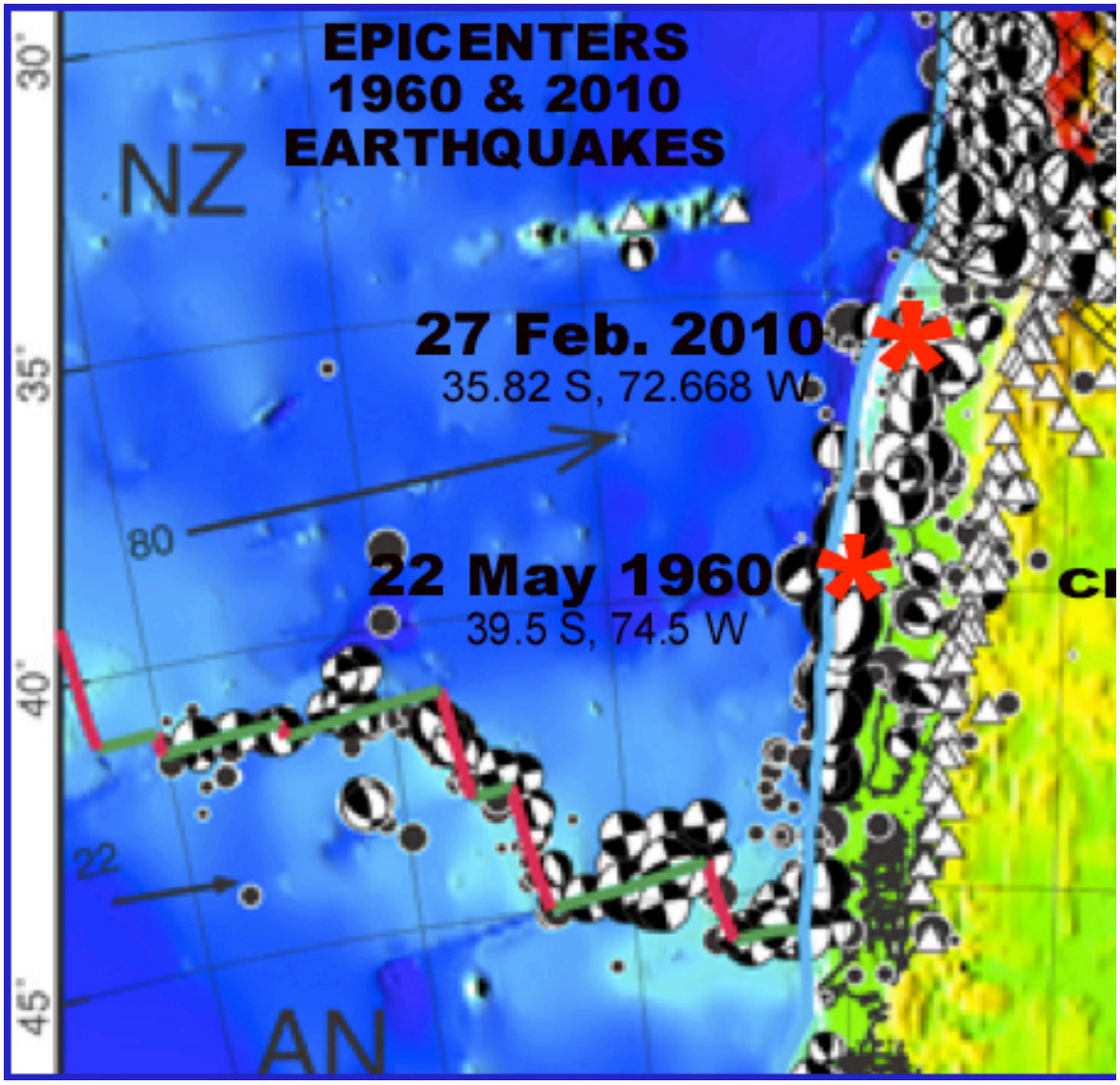

Fig. 11. Epicenters of the 27 February 2010 and of the 22 May 1960 earthquakes. Focal mechanisms of thrust faults on the coast of Chile and of tensional and compressive quakes on the Valdivia and the Juan Fernández Ridge, defining the extent of Chile's central seismic zone from 33^0-41^0 South (modified segment of Un. of Arizona graphic)

Earthquake Magnitudes **-** The great Chilean earthquake of May 22, 1960, was the largest seismic event ever recorded instrumentally in the world. The earthquake's moment magnitude (MW) was a staggering 9.5. The energy released was about one fourth of the total global seismic moment release between the years 1904-1986. A seismic moment of the 1960 quake was estimated at 2.7×10^{30} dyne-cm (Kanamori & Cipar, 1974), much greater than that of the 2010.

Foreshocks and Aftershocks - The 1960 earthquake was characterized by unusually long-period wave associated with a foreshock which occurred 15 minutes before the main shock, indicative of a large slow deformation in the epicentral area prior to the main failure (Kanamori & Cipar, 1974). The focal process resembled a large-scale deformation which begun gradually triggering first the foreshocks and then the main shock. No similar foreshock occurred with the 2010 earthquake, although it had an anomalously slow rupture.

Crustal Displacements - The 1960 earthquake affected an area estimated at 1.6×10^5 km^2. Other upper plate features that appear to correlate with earthquake slip may provide links to processes that occur on the megathrust. Wells et al. (2003) correlated the presence of forearc basins with locations of slip during great earthquakes. High slip during the 1960 earthquake occurred in the region of several forearc basins along that segment of the Chile margin (Bilek, 2009). The 2010 quake had with a maximum horizontal displacement of almost 10 meters. Comparison of aftershock distributions shows most of the crustal displacements of 2010 quake on land rather than in the ocean.

Rupture Lengths - The aftershock distribution of the 1960 earthquake indicates that its rupture was more than 1,000 km length and about 300 km in width and affected a much greater area. Its rupture velocity was 3.5 km/sec. The 2010 quake's rupture occurred immediately to the north of the segment ruptured by the great earthquake of 1960. It extended over 500 km in length and to depths of over 50 km below the earth's surface. The largest amount of its rupture occurred in the first 60 seconds, but smaller rupture displacements continued for up to 200 seconds.

Geometry of Subduction - Large earthquakes involve slip on a fault surface that is progressive in both time and space. Comparisons of focal hypocenters show differences in geometry of subduction near the surface and of dip along the Benioff zone. The 1960 quake had shallower angle of dip near the intersection of the Valdivia fracture zone with South America (Fig. 12) than the 2010 quake in the vicinity north of Concepción (Fig 13, 14). Based on synthetic seismograms a low-angle (10^0) thrust model was found to be consistent with the observed Rayleigh/Love wave ratio and the radiation asymmetry (Kanamori & Cipar, 1974).

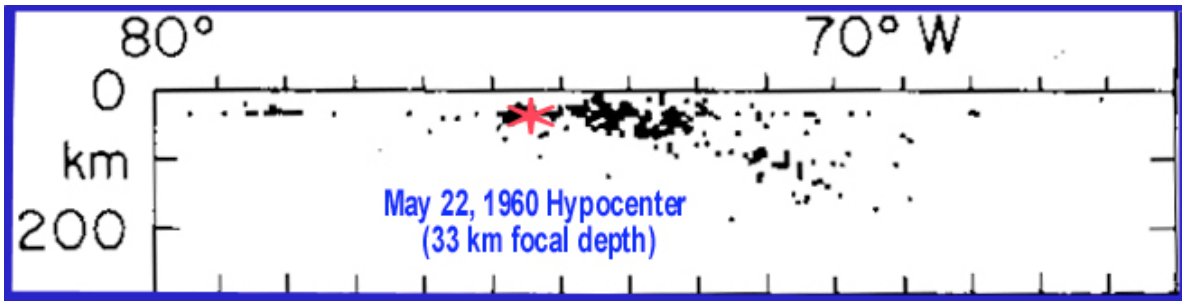

Fig. 12. Spatial distribution of aftershocks of the 1960 earthquake (refer)

An NEIS "map" of the slip on the fault surface of the 2010 Chilean earthquake (Fig. 7) shows how fault displacement propagated outward from an initial point (or focus) about 35

Km beneath the Earth's surface. Also the geometry of formation of the Valparaiso Basin and the aseismic subduction of the ridge seem to exhibit spatial patterns of earthquake ruptures and asperities in the 2010 affected region - something not occurring further south in the source region of the 1960 event.

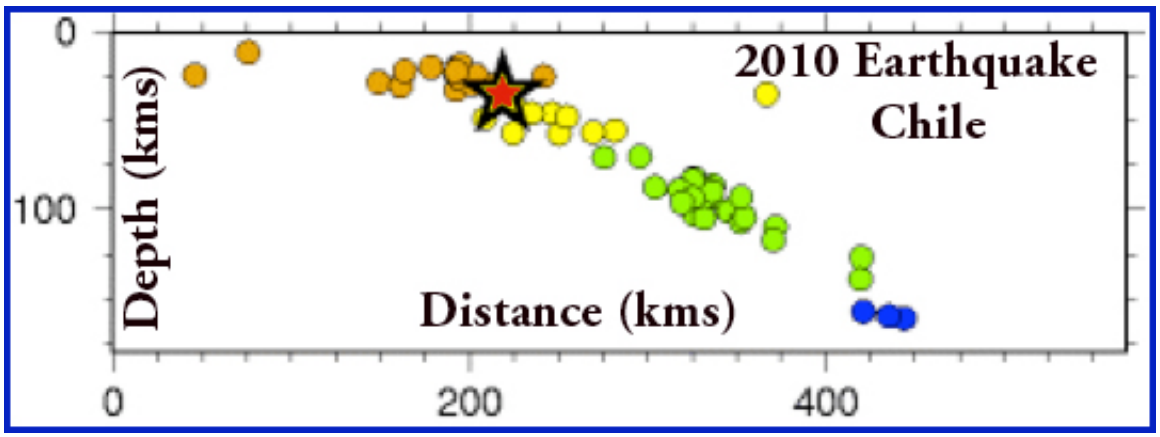

Fig. 13. Spatial distribution of aftershocks of the 2010 earthquake

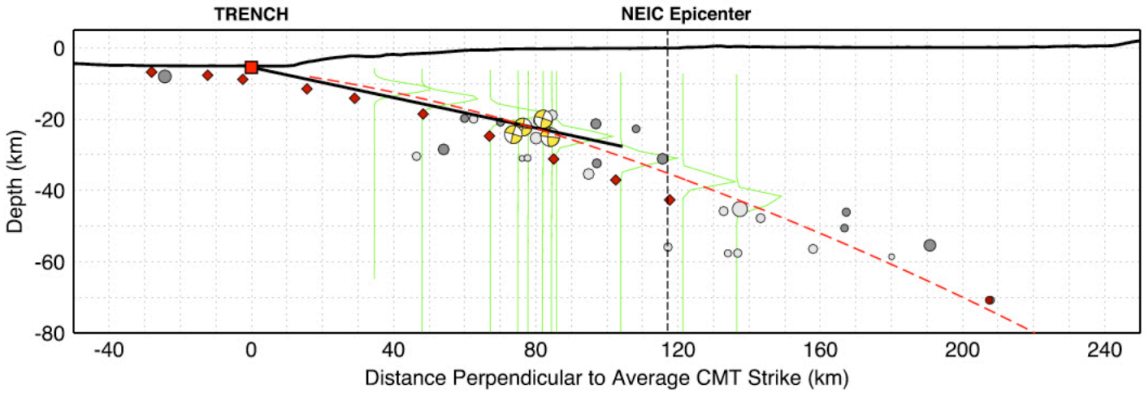

Fig. 14. Spatial distribution of aftershocks of the 2010 earthquake (modified NEIS graphic)

5.3 Comparison of Near and Far-field Tsunami Effects

Near-field effects **-** Given the 2010 earthquake's great magnitude (Mw8.8), greater near and far-field tsunami effects would have been expected. However, the 1960 tsunami had much greater near-field impact. Locally, the 1960 tsunami inflicted extensive damage in ten provinces of Chile. Waves ranging from 3 to 4 meters damaged the port of Lebu. Subsequent successive larger waves caused extensive destruction in Ancud, Bahia Mansa, Corral, Puerto Saavedra, and the coastal islands. Maximum tsunami height reached 14 meters in Maullin. At Caleta Mansa the first wave with a height of 8 meters, arrived 15 minutes after the quake. The second wave had a height of approximately 10 meters and the third was about 12 meters. Abnormal sea conditions continued for several days. Strangely, at Valparaiso the waves of greatest height were observed on 24 May – two days later. Local submarine topography and excitations of natural modes of oscillation (eigenmodes) of the Valparaiso basin may have been responsible for similar anomalies observed at different ports.

By contrast, the maximum tsunami wave heights of the 2010 tsunami observed of recorded locally in Chile, were significantly lower than those of 1960. Table 2 lists some of the heights of the two tsunamis as recorded by operating tide gauges in Chile.

Table 2. Tsunami wave heights in centimeters (above sea level) recorded at some tide gauges in Chile (San Juan Bautista is observed height)

LOCATION	2010	1960	LOCATION	2010	1960
Corral	144	1000	Valparaiso	261	170
Arica	118	220	Talcahuano	234	500
Caldera	90	290	Coquimbo	164	220
San Felix	79	NA	Constitución	200	250
Iquique	68	NA	San Juan Bautista	300	NA
Antofagasta	47	150			
San Pedro	40	NA			

Far-Field Effects **-** The far-field impact of the 1960 tsunami was much greater than that of 2010. The tsunami caused extensive destruction in Hawaii, Japan, Russia, New Zealand, Australia and elsewhere. The tsunami waves reached maximum height of 13 meters in the Pitcairn Islands, 12 meters in Hilo, Hawaii and up to 7 meters along some of Japan's coastline. By contrast, the 2010 tsunami had lesser amplitudes and caused only relatively small damage and no losses of lives. Table 2 summarizes some of the heights of the two tsunamis as recorded by selective operating tide gauges in the Pacific basin. Although heights recorded by tide gauges are not the maximum amplitudes of the waves that occurred on open coasts, they do indicate quantitatively the relative differences on the degree of tsunami impact.

Tsunami Energy Trapping, Reflection and Refraction **-** Some of the differences in near and far-field effects of the 1960 and 2010 tsunamis may have been caused by energy trapping and convergence by ducting, reflection and wave refraction. Given the orientation of the 2010 tsunami source and the directivity of maximum energy propagation, the Juan Fernández Juan Ridge, the O'Higgins seamount and other submarine features may have altered the tsunami's far-field impact by redirecting or deflecting its energy, thus resulting in the less significant far field effects that were observed. The submarine features may have trapped, channeled, refracted or reflected tsunami energy. Similar energy trapping by the Juan Fernández Submarine Ridge probably did not occur to the same degree with the 1960 tsunami because the generating source area was further south, was much larger and had different energy directivity. However, the Valdivia submarine ridge may have contributed to energy trapping and ducting of the 1960 tsunami towards the Southwest Pacific basin.

Table 3. Tsunami wave heights in centimeters (above sea level) recorded at some tide gauges in the Pacific.

LOCATION	2010	1960	LOCATION	2010	1960
Pago Pago, Am. Samoa	71	240	Callao, Peru	69	110
Winter Harbour, Canada	22	NA	Currimao, Philippines	16	NA
Rarotonga, Cook Islands	33	NA	Apia, Samoa	42	490
Santa Cruz, Ecuador La Libertad	105 NA	NA 190	King Cove	63	NA
Baltra, Galapagos	41	NA	Atka	42	NA
Rikitea, French Polynesia	32	NA	Seward	39	70
Hanasaki, Japan	95	NA	Shemya	39	NA
Ofunato	40	490	Kodiak	36	70
Naha	30	NA	Yakutat	36	80
Johnston Island	21	50	Craig, Alaska,	23	100
Saipan, Northern Marianas	15	NA	Santa Barbara	91	140
Midway Island	32	60	Crescent City	64	170
Acapulco	65.5	100	La Jolla	60	50
Cabo San Lucas, Mexico	35.9	75	Point Reyes, Calif.	46	NA
Gisborne	117	NA	Kahului	86	340
Chatham Island	101	NA	Kawaihae	51	270
Owenga	98	NA	Nawiliwili	40	150
Raoul Island, New Zealand	50	NA	Honolulu, Hawaii Hilo	26	80 1070

6. TSUNAMIGENIC EARTHQUAKES ALONG CHILE'S CENTRAL SEISMIC ZONE – FUTURE IMPACT

Combined oblique convergence, ridge collision and the subduction process play important roles in pre-seismic strain accumulation and must be taken into account in predicting future great tsunamigenic earthquakes along Chile's central seismic zone. The gradient in obliquity of convergence is also a significant factor in slip rates and crustal deformation and in the creation of forearc slivers, which may extend or contract parallel to the major tectonic arc. The build up in strain along this region of the subduction zone eventually requires release in the form of large horizontal and vertical crustal movements that restore temporarily isostatic balance. Thus, the February 27, 2010 earthquake and the numerous subsequent aftershock and independent events released substantial strain along the central seismic zone from about 33-37^0 South. Whether all the strain has been released further south is not known. However, based on the experience gained from the 2010 event, it is safe to conclude that future subduction earthquakes in this particular zone will generate tsunamis with destructive near-field impacts but with lesser far-field effects. The Juan Fernández Ridge, the O'Higgins seamount and other submarine features seem to alter a tsunami's far-field impact by redirecting or deflecting its energy, thus tsunamis generated in this segment do not result in very significant far-field effects.

However, this is not the case with the southern segment of the central zone (37^0-41^{0}S.) where the May 22, 1960 tsunamigenic earthquake occurred. The high seismicity of the Valdivia Ridge (Fig. 11) and the oblique plate convergence contribute significantly to the build up of strain in this southern segment. In the last five decades since 1960, crustal deformation from continuous plate convergence and subduction has been building strain in the region. Although some of the strain has been released partially by smaller events and some has been accommodated elastically, a great deal more is still accumulating. When the threshold limits of crustal elasticity are exceeded again in the region, another great earthquake can be expected. A tsunami similar to those generated by the 1960 and the 1575 earthquakes will have greater far-field tsunami impacts in the Pacific Basin. When such a great tsunami will occur again is very difficult to estimate with any degree of certainty at this time.

Estimating the recurrence frequencies of great earthquakes - based on slip rates - along the southern segment of Chile's central seismic region, is difficult. Apparently, the 1960 tsunamigenic earthquake ended a recurrence interval that had begun almost four centuries before in 1575. Two later earthquakes in 1737 and 1837 produced little subsidence or tsunamis and probably left a great deal of strain in this region from accumulated plate motion that the 1960 earthquake released subsequently (Cisternas et. al., 2005). Based on the intervals of the destructive earthquakes of 1575, 1737, 1837 and 1960, the recurrence frequency for the Valdivia segment has been estimated at 128 ± 31 yr.

Also, historic records of subduction earthquakes show that Isla Santa María is within the southern part of the Concepción seismic segment (Lomnitz, 1970; Barrientos, 1987; Beck et al., 1998; Campos et al., 2002), which nucleated M> 8 subduction tsunamigenic earthquakes in 1570, 1657, 1751 and 1835 (Lomnitz, 1970, 2004; Melnick et al., 2006). Fig. 15 is a cross-section at 37^0 South of the Nazca plate interaction with the South America continent across Isla Santa Maria and the Arauco Basin, just south of Concepción, which illustrates how faulting and oblique compression along the seismogenic

zone nucleates subduction, tsunamigenic earthquakes. Based on the historic events up to 1835, the recurrence of great earthquakes for this segment was estimated at 88 ± 5 yr (mean ±1σ standard deviation) (Melnick et al., 2006). However, if the 2010 event is included, the average recurrence shifts to 110 yrs intervals. For the Valparaiso segment immediately to the north – based again on historic events - the recurrence is estimated at about 82 ± 7 yr intervals.

Finally, it is quite possible that the strain release from the 2010 event may accelerate the recurrence of another great tsunamigenic earthquake along the southern segment of the central zone. It could occur in a few decades from now or much sooner along the same rupture zone as that of 1960. However, the use of new technology based on GPS geodetic measurements can help assess plate movements and slip rates. Such measurements may eventually lead to more accurate estimates of the recurrence frequency of great tsunamigenic earthquakes along Chile's central seismic zone.

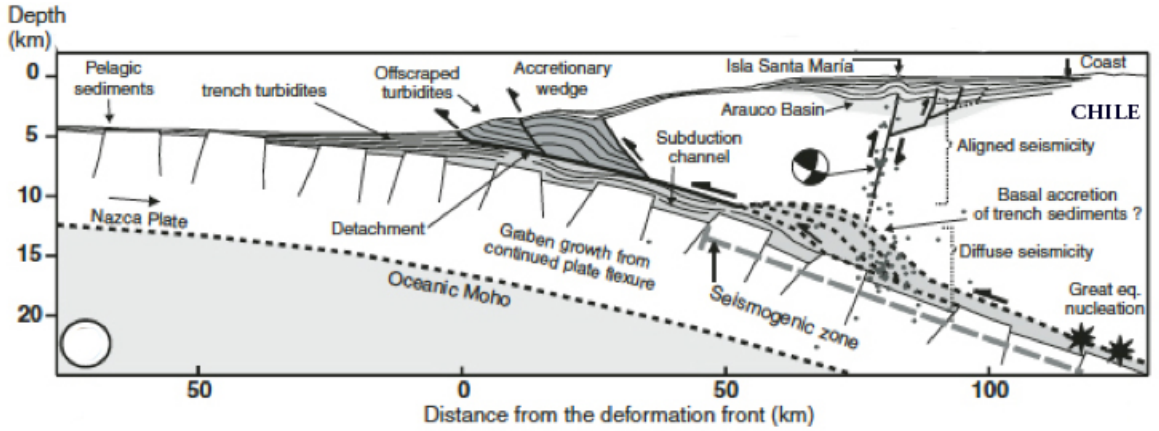

Fig. 15. *Cross-section at 37^0 South across Isla Santa Maria and the Arauco Basin, which illustrates how faulting and oblique compression along the Concepción seismogenic segment deforms the coastline and nucleates subduction-type of tsunamigenic earthquakes (modified after Melnick et al., 2006).*

7. SUMMARY AND CONCLUSIONS

Anomalous rupturing, clustering of aftershocks and slip distribution of earthquakes along the Nazca-South America convergence margin of Chile's central seismic region (33^0-41^0 South) are indicative of complexity in the moment release, which can be correlated to structural variations within the subducting and overriding plates. The anomalous interactions affect crustal displacements along this seismic zone and, therefore, the source characteristics of tsunamis that can be generated from large-scale, thrust and reverse thrust seismic events in the region - nucleated by offshore compressional earthquakes.

The February 27, 2010 earthquake occurred along a seismic gap along the region south of Valparaiso from about 34º South to 36º South of Chile's central seismic zone. The rupture connected directly to that of the great (M=9.5) 1960 tsunamigenic earthquake, which had its origin near Valdivia, immediately to the south. The anomalous, earthquake rupturing of the

2010 event in opposing directions probably has a diminishing effect on tsunami generating efficiency. The unusual clustering and chronological sequencing of aftershocks are indicative of a segmented and gradual release of tectonic stress. The unusual clustering in the spatial distribution of swarms of aftershocks which occurred near the Libertador O'Higgins and Bio-Bio regions following the main shock, appear to have acted as independent families of sequential seismic events. Energy may have been released gradually by such separate events on adjacent faults and this may partially account for observations of different degrees of inundation and tsunami directional approach as well as the lesser, far-field impact of the tsunami.

Evaluation of the source mechanism of tsunami generation associated with the earthquake of February 27, 2010 - as inferred from geologic structure, rupturing process, seismic intensities, spatial distribution of aftershocks, energy release and fault plane solutions - indicates that heterogeneous crustal displacements took place along the entire 550 km. earthquake rupture. As far as tsunami generation is concerned, such anomalous earthquake rupturing in opposing directions would be expected to have a diminishing effect on tsunami generating efficiency. Also, since more significant vertical displacements of the ocean floor occurred in the region north of Concepción, most of the tsunami energy was generated in this region. A good portion of this energy was trapped, ducted or reflected by prominent submarine features such as the Juan Fernández Ridge, the O'Higgins seamount - thus lessening the tsunami's far-field impact by redirecting or deflecting its energy. The crustal displacements and energy, which contributed to tsunami generation, need to be better determined and quantified.

Comparison of the source characteristics of the 1960 and of the 2010-tsunamigenic earthquakes show differences in energy release, geometry of subduction, angle of dip and extent of crustal displacements on land and in the ocean. Also, there were significant differences in coastal geomorphology, spatial distribution of hypocenters, clustering and time sequence of aftershocks and of seismic gaps at depth.

8. REFERENCES

Abe, K., Y. Sato, and J. Frez (1970). Free oscillations of the earth excited by the Kurile Islands earthquake 1963, *Bull. Earth. Res.* 48, 87-114.

Alsop, L. E., G. H. Sutton, and M. Ewing (1961). Free oscillations of the earth observed on strain and pendulum seisomographs, *J. Geophys. Res.* 66, 605-619.

Alsop, L. E. ,1964a. Excitation of free oscillations of the earth by the Kurile Islands earthquake of 13 October 1963. *Bull. Seism. Soc. Am.* 54, 1341-1348.

Alsop, L. E. 1964b. Spheroidal free periods of the earth observed at eight stations around the world, *Bull. Seism. Soe. Am.* 54, 755-776.

Barrientos, S., 1987. Is the Pichilemu-Talcahuano (Chile) a seismic gap?: Seismological Research Letters, v. 61, p. 43–48.

Beck, S., Barrientos, S., Kausel, E. and Reyes, M., 1998. Source characteristics of historic earthquakes along the central Chile subduction zone, *J. South American Earth Sci.* **11**(2), 115–129.

Benioff, H., F. Press, and S. Smith (1961). Excitation of the free oscillations of the earth by earthquakes, *J. Geophys. Res.* 66, 605 649.

Bilek S. L. , 2009. Seismicity along the South American subduction zone: Review of large earthquakes, tsunamis, and subduction zone complexity. Tectonophysics Journal, http://www.elsevier.com/locate/tecto

Bogert, B. P. (1961). An observation of the free oscillations of the earth, *J. Geophys. Res.* 66, 643-646.

Bolt, B. A.,1963. Revised torsional eigen periods from the 1960 Trieste data, *Geophys.* J. 7, 510-512.

Campos, J., Hatzfeld, D., Madariaga, R., López, G., Kausel, E., Zollo, A., Iannacone, G., Fromm, R., Barrientos, S., and Lyon-Caen, H., 2002, A seismological study of the 1835 seismic gap in south-central Chile: Physics of the Earth and Planetary Interiors, v. 132, p. 177–195, doi: 10.1016/S0031-9201(02)00051-1.

Cisternas M., Atwater B. F., Torrejón F., Sawai Y., Machuca G., Lagos M., Eipert A., Youlton C., Salgado I., Kamataki T., Shishikura M., Rajendran C. P., Malik J. K., Rizal Y. & Husni M., 2005. Predecessors of the giant 1960 Chile earthquake. *Nature* **437**, 404-407 (15 September 2005)

Connes, J., P. A. Blum, G. and N. Jobert,1962. Observations des oscillations propres de la terre, *Ann. Geophys.* 18,260-268.

Dziewonski, A. and M. Landisman,1970. Great circle Rayleigh and Love wave dispersion from 100 to 900 seconds, *Geophys. J.* 19, 37-91.

Fromm R., Alvarado P. , Beck S. L. & Zandt G., 2006. The April 9, 2001 Juan Fernandez Ridge (*M*w 6.7) tensional outer-rise earthquake and its aftershock sequence. Journal of Seismology (2006) 10: 163–170, Springer 2006.

Horrillo, J., Knight, W. and Kowalik Z. 2007. THE KURIL ISLANDS TSUNAMI of November 2006. Part II: Impact at Crescent City by local amplification (submitted to J. Geoph. Res.)

Iida, K., D.C. Cox, and Pararas--Carayannis, G., 1967. Preliminary Catalog of Tsunamis Occurring in the Pacific Ocean. Data Report No. 5. Honolulu: Hawaii Inst.Geophys. Aug. 1967.

Kanamori, H. and Cipar J.J., 1974. Focal Process of the Great Chilean Earthquake May 22, 1960. Physics of the Earth and Planetary Interiors, 9 (1974) 128-136. North-Holland Publishing Company, Amsterdam – Printed in the Netherlands.

Kowalik Z.,W. Knight, T. Logan and P. Whitmore (2005), Numerical modeling of the Global Tsunami: Indonesia Tsunami of 26 December 2004. *Science of Tsunami Hazards*, Vol. 23, No. 1, page 40-56. http://www.sfos.uaf.edu/tsunami/global/paper.pdf

Lomnitz, C., 1970. Major earthquakes and tsunamis in Chile during the period 1535 to 1955. Geologische Rundschau 59, 938–960.

Lomnitz, C., 2004. Major earthquakes of Chile: a historical survey, 1535–1960. Seismological Research Letters 75 (3), 368–378.

McCann, W.R., Habermann, R.E., 1989. Morphologic and geologic effects of the subduction of bathymetric highs. Pure and Applied Geophysics 129 (1–2), 41–69.

Melnick D., Bookhagen B., Echtler H. P. & Strecker M. R., 2006. Coastal deformation and great subduction earthquakes, Isla Santa María, Chile (37°S), *GSA Bulletin*; November 2006; v. 118; no. 11-12; p. 1463-1480

Ness, N. F., J. C. Harrison, and L. B. Slichter (1961). Observations of the free oscillations of the earth, *J. Geophys. Res.* 66, 621-629.

Nowroozi, A. A.,1965. Eigen vibrations of the earth after the Alaskan earthquake, *J. Geophys. Res.* 70, 5145-5156.

Nowroozi, A. A., 1966. Terrestrial spectroscopy following the Rat Islands earthquake, *Bull. Seism. Soc. Am.* 56, 1269-1288.

Nowroozi, A. A. and L. E. Alsop (1968). Torsional free periods of the earth observed at six stations around the earth, *Nuovo Cimento, Ser. 1, Suppl.* 6, 133-146.

Newsolio. 2010-02-27. 40 Meter Tsunami Wave Hits Juan Fernández Island". Retrieved 27 February 2010.

Pararas-Carayannis, G., 1968. Catalog of Tsunamis in the Hawaiian Islands. Data Report Hawaii Inst.Geophys. Jan. 1968

Pararas-Carayannis, G. and Calebaugh P.J., 1977. Catalog of Tsunamis in Hawaii, Revised and Updated , World Data Center A for Solid Earth Geophysics, NOAA, 78 p., March 1977.

Pararas-Carayannis, G., 2005. Earthquake and Tsunami of December 26, 2004, in Indonesia http://drgeorgepc.com/Tsunami2004Indonesia.html

Pararas-Carayannis, G., 2007. Earthquakes and Tsunami of September 12, 2007, in Indonesia http://drgeorgepc.com/Tsunami2007Indonesia.html

Rehak K., Strecker M.R., and Echtler H P., 2008. Morphotectonic segmentation of an active forearc, 37°–41°S, Chile. Geomorphology 94 (2008) 98–116,

Slichter, L. B.,1967. Spherical oscillations of the earth, *Geophys. J.* 14, 171-177.

Smith, S. W.,1966. Free oscillations excited by the Alaskan earthquake, *J. Geophys. Res.* 71, 1183-1193.

Spinali, G., 2010. "40 Meter Tsunami Wave Smashes Juan Fernandez Island". Hollywood Backstage. Retrieved 27 February 2010.

Tinti, S. and Vannine C., 1995. Tsunami Trapping Near Circular Islands, PAGEOPH, Vol. 144, Nos. ¾ (1995), Birkhauser Verlag, Basel.